

雷射鑽孔過程的熱效應

Thermal Effect of the Laser-Drilling Processes

黃廣志·許隆勝 Kuang-Chih Huang and Long-Sheng Hsu

Department of Electrophysics, N.C.T.U.

(Received August 30, 1976)

ABSTRACT — A model that uses a continuous, distributed, and moving heat source to describe the temperature profile for laser-drilled-holes has been developed. A new mathematical approach has been systematically performed in detail. The temperature profile of the laser-formed hole are calculated to indicate the magnitude of those factors that can influence the processes of the removal of materials. A modified CO₂ laser system, based on double-pulse-discharge technique [1], has been set up. Using this modified laser system, the experimental results are found to be in agreement with the mathematical analysis.

I. Introduction

Heat flow in a material has been treated for the case of electromagnetic radiation from an intense laser source impinging on and being absorbed by the surface of the material. Several thermally induced effects are observed [2, 3]. An understanding of these effects is of great importance for laser-drill-
ed process and industrial applications of lasers.

Solutions to this problem are given as temperature profiles for a three-dimensional heat-conduction model. To simplify the mathematics, the focused beam is taken as a continuous, distributed, and moving source in the direction of beam axis. Previously, reported works have only treated the problem roughly. The boundary and initial conditions of the partial differential equation have been dealt intuitively. And the most mathematical works are left for computer. The results are only quantitatively computerized-figures.

This paper deals with the problem systematically. The Green's function is applied based on the initial condition and boundary condition of the heat conduction differential equation. After the strict mathematical derivation, we believe this is the first explicit mathematical expression for the drilled-shape that already took into account some parameters such as power density, pulse duration, pulse waveform, focused beam diameter, material thermal coefficients, and initial temperature, etc.

The self-designed CO₂ laser system has raised the laser pulse energy by a factor of 6.5 compared to our older laser set-up [1]. Using this new-design-

ed laser, we found that the experimental results are in agreement with the derived-formula.

II. Thermal Analysis of Laser-Induced Vaporization

In order to set up the problem, we shall first consider whether we are justified in using conventional methods for calculating heat transfer under conditions which are so far removed from what is usual. Now the question is whether the temperature a meaningful concept in a situation which is far from equilibrium.

In general, the mean free time between collisions for electrons is of the order of 10^{-14} to 10^{-13} sec. Thus for times of the order of 10^{-9} sec, the shortest time intervals with which we will be concerned, the electrons will have made many collisions both among themselves and with lattice phonons. Since these collision processes govern the processes of heat transfer. So the laser energy is instantaneously converted to heat at the point at which the light was absorbed. A local equilibrium can be established rapidly enough among electrons and phonons that temperature should remain a valid concept. Relying on this justification, we would assume the applicability of the usual equation for heat flow.

In order to make the problem manageable, we will make several further assumptions referred to references: [2] [3] [4] and [5]

(1) The thermal constants such as thermal conductivity K , specific heat C , and mass density ρ , are independent of both the laser beam intensity and the temperature.

(2) The optical absorption coefficient is large, corresponding to the case in which the absorption of the incident radiation to make heat generation takes place in the surface plane of the material.

(3) The gas that is created due to the vaporization of the material is transparent to the incident laser energy.

(4) The effect of the liquid phase can be ignored. Because the latent heat of fusion of a typical material is much smaller than either the latent heat of vaporization or the quantity of heat required to raise to boiling point.

1. Mathematical Model

Under the prescribed assumptions, the laser vaporization problem can be described by the heat conduction equation.

$$\frac{\partial T}{\partial t} = k\nabla^2 T \quad (1)$$

where T temperature
 t : time

- $k=K/\rho c$: thermal diffusivity
- ρ : mass density
- C : specific heat
- K : thermal conductivity

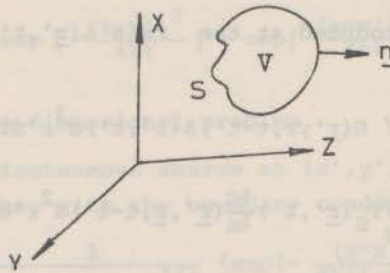


Fig. 1

According to the above diagram, the solid is bounded by the surface S . Its volume is V . The Green's function G is taken as the temperature at $P(\underline{r})$ at time t due to an instantaneous point source of unit strength generated at $P(\underline{r}')$ at time t' , where $t' < t$, together with two following conditions being satisfied.

- (1) the solid initially at zero temperature except at $P(\underline{r}')$.
- (2) the surface S being kept at zero temperature.

Then the problem can be expressed mathematically as follows:

$$\frac{\partial G(\underline{r}, \underline{r}', t-t')}{\partial t} = k \nabla^2 G(\underline{r}, \underline{r}', t-t'), t > t' \tag{2}$$

$$G(\underline{r}, \underline{r}', 0) = 0, \quad \underline{r} \text{ is } S, r \neq r'$$

$$G(\underline{r} \text{ at } S, r', t-t') = 0$$

Let function $T(\underline{r}, t)$ denote the temperature at time t due to the initial temperature $T_0(\underline{r}, 0)$ and surface temperature $T_s(\underline{r}, t)$.

$$\frac{\partial T(\underline{r}, t)}{\partial t} = k \nabla^2 T(\underline{r}, t), \quad t > 0 \tag{3}$$

$$T(\underline{r}, t=0) = T_0(\underline{r}, t), \quad \underline{r} \text{ in } S$$

$$T(\underline{r} \text{ at } S, t) = T_s(\underline{r}, t)$$

$$\begin{aligned} \iiint_V \frac{\partial}{\partial t} (GT) d^3r &= \iiint_V k(G \nabla^2 T - T \nabla^2 G) d^3r \\ &= k \iint_S (G \frac{\partial T}{\partial n} - T \frac{\partial G}{\partial n}) d^2r \end{aligned} \tag{4}$$

$$\lim_{\epsilon \rightarrow 0} \int_0^{t-\epsilon} \iiint_V \frac{\partial}{\partial t} (GT) d^3r dt' = \lim_{\epsilon \rightarrow 0} \int_0^{t-\epsilon} \iint_S k (G \frac{\partial T}{\partial n} - T \frac{\partial G}{\partial n}) d^2r dt' \tag{5}$$

By changing the variables $\underline{r} \rightarrow \underline{r}'$, $\underline{r}' \rightarrow \underline{r}$, we then obtain the important results.

$$T(\underline{r}, t) = \iiint_V G(\underline{r}', \underline{r}, t) T(\underline{r}', 0) d^3 r' - k \int_0^t \iint_S T_S(\underline{r}', t') \frac{\partial G(\underline{r}', \underline{r}, t-t')}{\partial n} d^2 r' dt' \quad (6)$$

If heat source is produced at the rate $A(\underline{r}', t')$ continuously when $t' > 0$. The complete solution is

$$T(\underline{r}, t) = \int_0^t \iint_V G(\underline{r}', \underline{r}, t-t') A(\underline{r}', t') d^3 r' dt' + \iiint_V G(\underline{r}', \underline{r}, t) T(\underline{r}', 0) d^3 r' - k \int_0^t \iint_S T_S(\underline{r}', t') \frac{\partial G(\underline{r}', \underline{r}, t-t')}{\partial n} d^2 r' dt' \quad (7)$$

2. The Selection of Green's Function for Laser-Vaporization

Step 1. The Green's function G_1 for a unit instantaneous source at $t'=0$ at position X' in infinite line would be expressed as

$$G_1 = \frac{1}{2(\pi kt)^{1/2}} \exp[-(x-x')^2/4kt] \quad (8)$$

Step 2. Unit instantaneous source at $t'=0$ at $t'=0$ at position X' in semi-infinite line $X > 0$, and no heat flow at $X=0$ are assumed.

The solution of the problem can be obtained by the linear superposition of two Green's functions.

$$G = G_1 + G_2$$

where G_2 also satisfies the equation of heat conduction.

$$\frac{\partial^2 G_2}{\partial x^2} - \frac{1}{k} \frac{\partial G_2}{\partial t} = 0$$

Taking the Laplace transformation,

$$\begin{aligned} L\{G_1(t)\} &= \int_0^\infty e^{-st} \frac{1}{2(\pi kt)^{1/2}} \exp[-(x-x')^2/4kt] dt \\ &= \frac{1}{2\sqrt{ks}} \exp(-\sqrt{\frac{s}{k}} |x-x'|) \end{aligned} \quad (9)$$

$$\frac{\partial^2 [L(G_2)]}{\partial x^2} - \frac{s}{k} L(G_2) = 0$$

$$L(G_2) = C \exp[-\sqrt{\frac{s}{k}} x] \quad (10)$$

where C is constant which will be determined. To substitute into the boundary

condition.

$$\frac{\partial L(G)}{\partial x} = 0 \quad \text{at } x=0,$$

Thus,
$$L(G) = \frac{1}{2\sqrt{ks}} \exp(-\sqrt{\frac{s}{k}} |x-x'|) + \frac{1}{2\sqrt{ks}} [\exp -\sqrt{\frac{s}{k}} (x+x')]$$

$$G = \frac{1}{2\sqrt{\pi kt}} \left\{ \exp \left[-\frac{(x-x')^2}{4kt} \right] + \exp \left[-\frac{(x+x')^2}{4kt} \right] \right\} \quad (11)$$

Step 3. To extend to three-dimensional problem.

By taking an unit instantaneous source at (x', y', z') at time t' for semi-infinite solid $x > 0$, together with the boundary condition $\frac{\partial G}{\partial x} = 0$ at $x=0$.

$$G(\underline{r}, \underline{r}', t-t') = \frac{1}{8[\pi k(t-t')]^{3/2}} \left\{ \exp \left[-\frac{(x-x')^2}{4k(t-t')} \right] + \exp \left[-\frac{(x+x')^2}{4k(t-t')} \right] \right\} \cdot \exp \left[-\frac{(y-y')^2 + (z-z')^2}{4k(t-t')} \right]$$

Substituting in equation (7); and noting that $\frac{\partial G}{\partial n} = 0$ at $x=0$. While the initial solid temperature is applicably assumed constant, i.e., $T(\underline{r}', 0) = T_0$

The equation (7) then reduces to

$$T(\underline{r}, t) = T_0 + \int_0^t \iiint_V G(\underline{r}, \underline{r}', t-t') A(\underline{r}', t') d^3 r' dt' \quad (13)$$

For spatial-uniform disc laser beam (In fact, it's the Gaussian spatial distribution for TEM₀₀ mode).

Refer the following diagram, the laser heat source can be expressed as:

$$A(\underline{r}', t') = \frac{P(t') \delta(x')}{\rho c} \quad , \text{ for } r' \leq a$$

$$= 0 \quad , \text{ for } r' > a$$

where $P(t')$ is laser power density at t' , $2a$ is beam spot size.

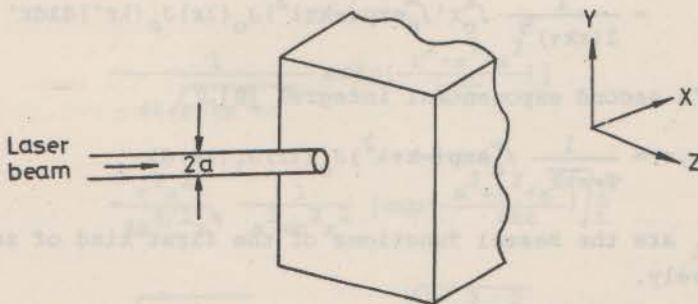


Fig. 2

Taking the polar coordinates, and let $t-t'=\tau$.

$$\begin{aligned}
 (z-z')^2+(y-y')^2 &= r^2+r'^2-2rr'\cos(\theta-\theta') \\
 T(\underline{r},t) &= T_0 + \frac{1}{\rho c} \int_0^t P(t') \int_0^a \frac{r'}{8(\pi k \tau)^{3/2}} \exp\left(-\frac{r^2+r'^2}{4k\tau}\right) \\
 &\quad \cdot \left[\exp\left(-\frac{(x-x')^2}{4k\tau}\right) + \exp\left(-\frac{(x+x')^2}{4k\tau}\right) \right] \\
 &\quad \cdot \int_0^{2\pi} \exp\left[-\frac{2rr'\cos(\theta-\theta')}{4k\tau}\right] d\theta' dr' d\tau \\
 &= T_0 + \frac{1}{\rho c} \int_0^t P(t') \int_0^a \frac{r'}{4\sqrt{\pi}(k\tau)^{3/2}} \left[\exp\left(-\frac{(x-x')^2}{4k\tau}\right) \right. \\
 &\quad \left. + \exp\left(-\frac{(x+x')^2}{4k\tau}\right) \right] \cdot \exp\left(-\frac{r^2+r'^2}{4k\tau}\right) I_0\left(\frac{2rr'}{4k\tau}\right) dr' d\tau \quad (14)
 \end{aligned}$$

Here I_0 is the modified zero-order Bessel function of the first kind.

Due to the vaporization of material, the heat source is moving actually. So equation (14) must be modified. Now, the source position is the function of time. We simply change the variable $x' \rightarrow x'(t')$. Further more, conservation of energy at the moving interface requires that the energy given to the vaporized materials is equal to the energy conducted from the solid.

$$\rho L_V x'(t') = K \frac{\partial T}{\partial x} \quad (x \text{ at material interface}) \quad (15)$$

where L_V is latent heat of vaporization.

Then, the complete theoretical derivation comes the result:

$$\begin{aligned}
 T(\underline{r},t) &= T_0 + \int_0^t \frac{1}{\rho c} \int_0^a P(t') \left[\exp\left(-\frac{[x-x'(t')]^2}{4k\tau}\right) \right. \\
 &\quad \left. + \exp\left(-\frac{[x+x'(t')]^2}{4k\tau}\right) \right] F(r,\tau) dr' d\tau \quad (16)
 \end{aligned}$$

where notation $F(\underline{r},\tau)$ is

$$\begin{aligned}
 F(r,\tau) &= \int_0^a \frac{r'}{4\sqrt{\pi}(k\tau)^{3/2}} \exp\left(-\frac{r^2+r'^2}{4k\tau}\right) I_0\left(\frac{2rr'}{4k\tau}\right) dr' \\
 &= \frac{1}{2(\pi k \tau)^{3/2}} \int_0^a r' \int_0^\infty \exp(-k\tau\lambda^2) J_0(\lambda r) J_0(\lambda r') d\lambda dr'
 \end{aligned}$$

Which is Weber's second exponential integral [9].

$$F(r,\tau) = \frac{1}{2\sqrt{\pi k \tau}} \int_0^\infty \exp(-k\tau\lambda^2) J_0(\lambda r) J_1(\lambda a) d\lambda \quad (17)$$

where J_0 and J_1 are the Bessel functions of the first kind of zero and first order respectively.

The asymptotic estimation of $F(r,\lambda)$ would be obtained under the different

cases.

It is reasonable to simplify the laser waveform as the equivalent rectangular shape. In mathematical words, we assumed

$$P(t') = P_0, \quad 0 \leq t' \leq t$$

$$P(t') = 0, \quad \text{otherwise}$$

When the laser-beam possesses sufficient power, the vaporization may occur. Then the temperature profile should be solved by iterative method except on the plane $x=0$.

Case 1. $x=0, \quad kt \geq 2a^2$

$$T(\underline{r}, t) = T_0 + \frac{2P_0}{\rho c} \left\{ \left(\frac{t}{\pi k}\right)^{\frac{1}{2}} (1 - \exp(-\frac{a^2}{4kt})) + \frac{a}{2k} \operatorname{erfc}\left(\frac{a}{\sqrt{4kt}}\right) - \frac{r^2}{8k \frac{3}{2} \pi^{\frac{1}{2}}} \left[\frac{\sqrt{t}}{t} \exp(-\frac{a^2}{4kt}) + \frac{\sqrt{\pi k}}{a} \operatorname{erfc}\left(\frac{a}{\sqrt{4kt}}\right) \right] \right\}$$

where $\operatorname{erfc}(x) = \frac{1}{\sqrt{\pi}} \int_x^\infty \exp(-\xi^2) d\xi$ Formula (I)

Case 2. $x=0, \quad kt \leq \frac{a^2}{4}$

$$T(\underline{r}, t) = T_0 + \frac{P_0}{\rho c} \cdot \frac{1}{\pi \sqrt{ar}} \left[t \exp(-\frac{(r-a)^2}{4kt}) - E_i(-\frac{(r-a)^2}{4kt}) \frac{(r-a)^2}{4k} \right]$$

where $-E_i(-x) = \int_x^\infty \frac{1}{u} \exp(-u) du$ Formula (II)

Case 3. $\frac{a^2}{4} \leq kt \leq 2a^2,$

$$T(\underline{r}, t) = T_0 + \frac{2P_0}{\rho c} \left\{ \left(\frac{t}{\pi k}\right)^{\frac{1}{2}} \exp(-\frac{r^2+x^2}{4kt}) [1 - \exp(-\frac{a^2}{4kt})] - \frac{\sqrt{x^2+a^2}}{2k} \operatorname{erfc}\left(\frac{\sqrt{x^2+a^2}}{\sqrt{4kt}}\right) + \frac{\sqrt{x^2+r^2+a^2}}{2k} \operatorname{erfc}\left(\frac{\sqrt{x^2+r^2+a^2}}{\sqrt{4kt}}\right) + r^2 \left[\frac{1}{4k\sqrt{r^2+x^2}} \operatorname{erfc}\left(\frac{\sqrt{r^2+x^2}}{\sqrt{4kt}}\right) - \frac{1}{4k\sqrt{r^2+x^2+a^2}} \operatorname{erfc}\left(\frac{\sqrt{r^2+x^2+a^2}}{\sqrt{4kt}}\right) \right] - \frac{r^2 a^2}{8k \frac{3}{2} \pi^{\frac{1}{2}}} \frac{1}{a^2+r^2 x^2} \left[\exp(-\frac{a^2+r^2+x^2}{4kt}) \sqrt{\frac{1}{t}} + \sqrt{\frac{\pi k}{a^2+x^2+r^2}} \cdot \operatorname{erfc}\left(\frac{\sqrt{a^2+r^2+x^2}}{\sqrt{4kt}}\right) \right] \right\}$$

Formula (III)

Case 4. $r=0$

$$T(\underline{r}, t) = T_0 + \frac{P_0}{\rho c} \sum_{m=0}^n \frac{\Delta t}{2[\pi k(t-m\Delta t)]^{\frac{1}{2}}} \cdot [1 - \exp(-\frac{a^2}{4k(t-m\Delta t)})] \cdot \{ \exp[-\frac{(x-x')(m\Delta t)^2}{4k(t-m\Delta t)}] + \exp[-\frac{(x+x')(m\Delta t)^2}{4k(t-m\Delta t)}] \} \quad \text{Formula (IV)}$$

Case 5. $x \neq 0, r \neq 0$

$$T(\underline{r}, t) = T_0 + \frac{P_0}{\rho c} \sum_{m=0}^n \Delta t \cdot F(\underline{r}, t-m\Delta t) \{ \exp[-\frac{(x-x')(m\Delta t)^2}{4k(t-m\Delta t)}] + \exp[-\frac{(x+x')(m\Delta t)^2}{4k(t-m\Delta t)}] \} \quad \text{Formula (V)}$$

where $x'(M\Delta t)$ merely represents the vaporization interface position at time $t=m\Delta t$.

III. Experiments

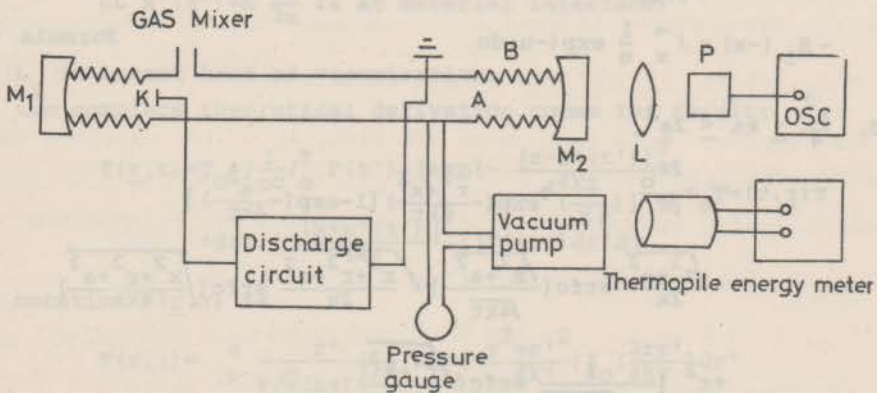


Fig. 3. Block diagram of the experimental equipments.

M_1 : 100% Reflector, Radius of curvature=10m

M_2 : 50% Reflector, Radius of curvature=10m

L : 10.6 μ laser focusing lens

K : Cathode

A : Anode

B : Bellow

P : Photon-Drage Detector

The block diagram of the experimental set-up is shown in Fig.3. The laser

tube is a 190 cm-long, 35 mm-bore pyrex tube. The discharge cavity has the length of 120 cm. A gold coated mirror with 2 mm-hole at the center and 10m radius of curvature was used as 100% reflector. The 2mm-hole was used to align the optical cavity with a He-Ne laser. The output mirror is a Ge 50%-transmission reflector. The laser beam energy was measured by a HADRON/energy/power meter. The laser pulse waveform was detected by a CO₂ photodrag detector [8]. The display was stored by Technics 7623 Oscilloscope. The discharge circuit is shown as Fig. 4, which is two-stage double-pulse-discharge excitation technique [1].

The new discharge technique consists in producing two consecutive discharges: The first one is obtained from a very small of energy (capacitor C_p) and serves to preionize the gas. While the more abundant uniform plasma well distributed along the cavity, the second or main discharge, much more energetic, (Capacitor C_s) then takes place. Since the low energy preliminary discharge can be produced from a very small capacitor, the time constant can be kept short and it is easier to excite electrode without causing arcing.

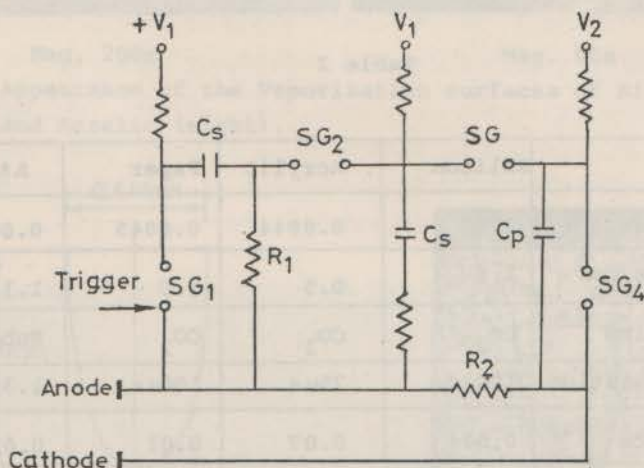


Fig. 4. Schematic of two-stage double-pulse-discharge excitation circuit.

C_s-Energy storage capacitor, 0.02μF

C_p-Preionization capacitor, 500PF

SG₁, SG₂, SG₃, SG₄-Controlled spark gaps

The summary of laser energy data is shown in Table 1.

Table 1

Excitation system	Storage capacitor	0.02μF
Characteristics	Preionization capacitor	500PF
	Voltage supply V ₁	32KV
	Voltage supply V ₂	12.5KV

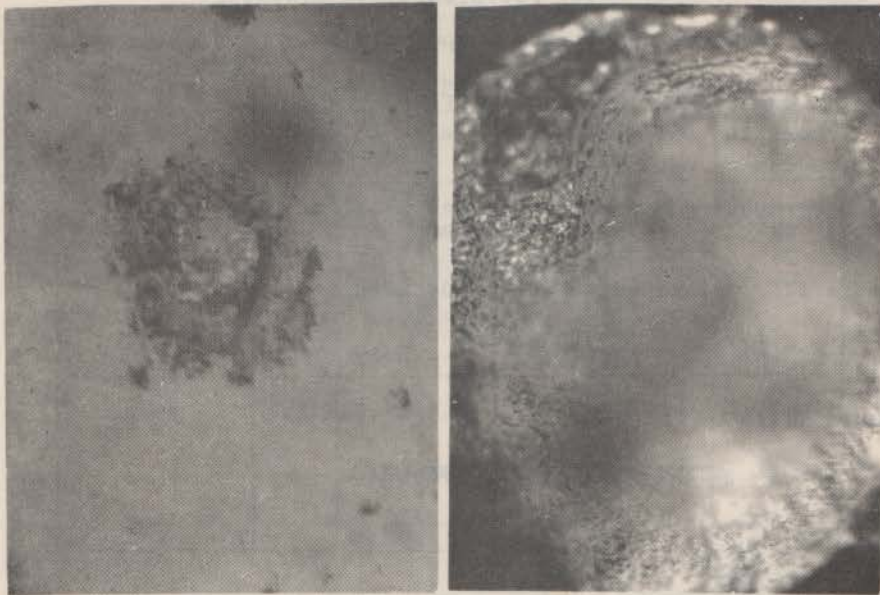
	Input energy	20.48J/pulse
Discharge Characteristics	Active length	120cm
	Tube bore	3.3cm
	Excited volume	1027cm ³
	Input energy density	20mJ/cm ³
	Total pressure	30torr
	CO ₂ :N ₂ :H _e	10:7:15
Output	Energy	1.8J/pulse
Characteristics	Over-all efficiency	8.8%
	E/P	8.9V/cm-torr

IV. The Laser-Drilled Experiments

Now, we are taking four material as sample drilled corresponding to each different laser source condition. The following table and figure show us that the Formuladerived is considerable in agreement with the experimental data.

Table 2

Material	Silicon	Acrylic	Paper	Al ₂ O ₃
K cm ² /sec	0.53	0.0044	0.0045	0.06
ρC joule/cm ³	1.6	0.5	5.0	1.14
Laser Kind	CO ₂	CO ₂	CO ₂	Ruby
Pulse duration	100μs	75μs	100μs	1.38 ms
Spot Size, cm	0.006	0.07	0.01	0.012
Power, watt/cm ²	2.8x10 ⁷	5.6x10 ⁶	10 ⁷	3.2x10 ⁷
Formula-used	Formula (III)	Formula (II)	Formula (II) (IV)	Formula (V)
hole radius -calculated cm	0.011cm	0.073	0.013	0.044
experimetal hole radius cm	0.010cm	0.069	0.012	0.041
hole depth calculated cm	————	————	0.029	0.075
experimental hole depth cm	————	————	0.025	0.071



Mag. 200x

Mag. 80x

Fig. 5. Appearance of the Vaporization surfaces of Silicon (left) and Acrelic (right).

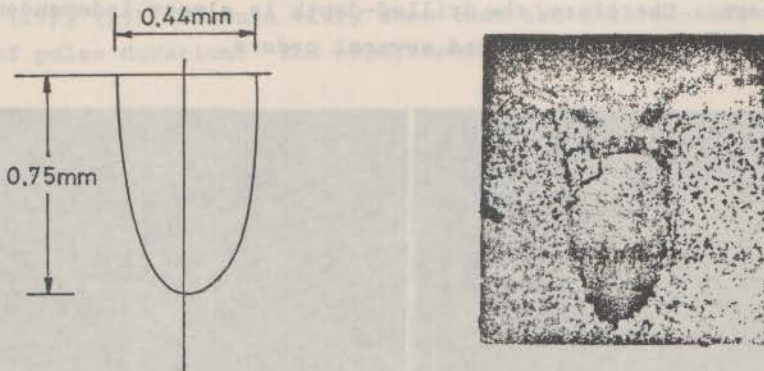


Fig. 6. Predicted Shape (left), Experimental shapedrilled (right) which diameter-0.41mm, depth-0.71mm Mag. 50x, [3].

(1) The vaporized-threshold power density P_t , energy W_t . From Formula (I), it is easily proved that

$$P_t = \frac{\rho C T_v}{2} \left[\left(\frac{t}{\pi k} \right)^{\frac{1}{2}} [1 - \exp(-\frac{a^2}{4kt})] + \frac{a}{2k} \operatorname{erfc} \left(\frac{a}{\sqrt{4kt}} \right) \right]^{-1} \quad (18)$$

where equivalent vaporization temperature T_v .

$$T_v = T_b + \frac{L_v}{C}$$

$$W_t \approx P_t \pi a^2 \cdot t$$

It's the function of spot size, pulse duration strongly.

(2) Effect of power density on shape-drilled.

Let
$$A = \left(\frac{t}{\pi k}\right)^{\frac{1}{2}} \left[1 - \exp\left(-\frac{a^2}{4kt}\right)\right] + \frac{a}{2k} \operatorname{erfc}\left(\frac{a}{\sqrt{4kt}}\right)$$

$$B = \frac{1}{8k^{3/2} \pi^{\frac{1}{2}}} \left[\sqrt{\frac{1}{t}} \exp\left(-\frac{a^2}{4kt}\right) + \frac{\sqrt{\pi k}}{a} \operatorname{erfc}\left(\frac{a}{\sqrt{4kt}}\right) \right]$$

From Formula (I), drilled-size can be derived as:

$$S \cong \frac{1}{B} \left[A - \frac{\rho C (T_v - T_o)}{2P_o} \right]^{\frac{1}{2}} \quad (19)$$

From Formula (II)

$$S \cong a + \sqrt{-4kt \ln \left[\frac{\rho C (T_v - T_o)}{P_o T} \right]} \quad (20)$$

In general, $A \gg \frac{T_v \rho C}{2P_o}$

So the drilled-size is almost independent of power density.

The penetration depth can be seen from Formula (IV). The temperature function is dominated by exponential term $\exp[-(X-X')^2/4k(t-m\Delta t)]$, not dominated by P_o term. Therefore, the drilled-depth is almost independent of power density when P_o doesn't vary beyond several orders.

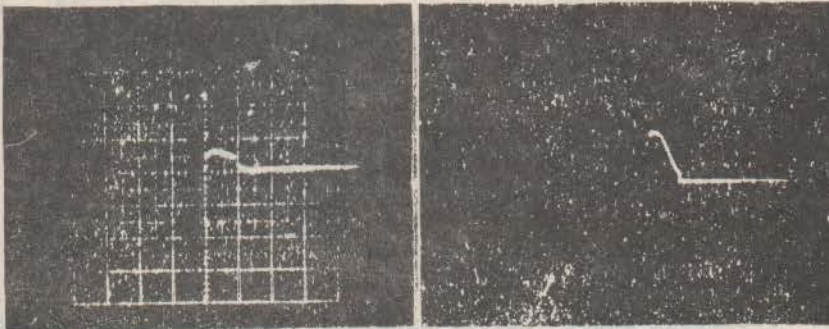


Fig. 7. CO_2 laser pulse 1 (left) duration=50 μs energy=0.7 joules pulse 2 (right) duration=50 μs , energy=1.57 joules.

The above figures show that two laser pulses have different pulse energy. The experimental table shows that the drilled-shape due to two different power density have identical shape.

Table 3

Experimental data Material	Pulse 1		Pulse 2		Pulse 1,2	
	a	P ₀	a	P ₀	drilled size	drilled depth
glass	0.15 mm	1.4x 10 ⁷ w/cm ²	0.15 mm	3.2x 10 ⁷ w/cm ²	0.16mm	—
paper	0.1 mm	3.15 x10 ⁷ W/cm ²	0.1 mm	7.2 x10 ⁷ W/cm ²	0.11mm	0.15mm

The tangential stress of these laser pulse is beyond the maximum tangential stress tolerance of the glass. The crack of the glass made the measurement of drilled depth impossible.

(3) Effect of pulse duration on shape-drilled.

Equations (19), (20), Formula (IV), show that the drilled-shape is the strong function of pulse duration. The experimental verification is shown in Table 4 and 5.

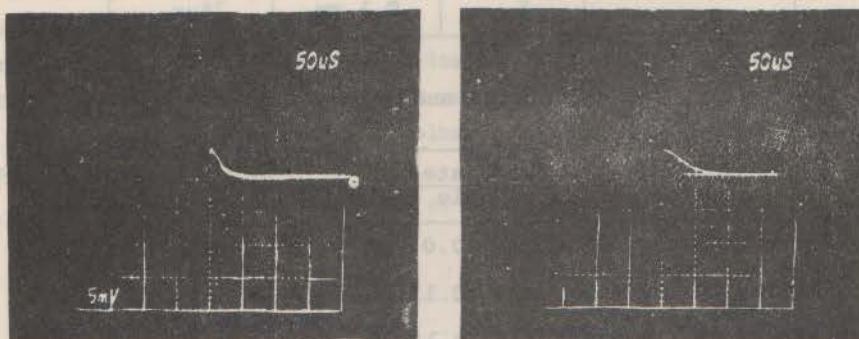


Fig. 8. Laser pulse 3, duration=25μs, Fig. 9 pulse 4, duration=50μs.

(4) Effect of initial temperature on shape-drilled.

The Formula (IV), Equation (19), (20) also show the influence of initial temperature would be neglected. The initial temperature of material thus have no effect on the shape-drilled.

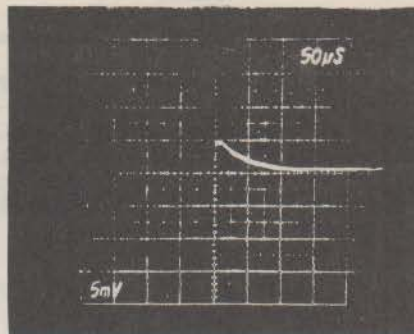
Fig. 9. Laser pulse 5, duration=75 μ s.

Table 4. Experimental parameter

Experimental parameter Material	Pulse number	a	Pulse duration
Acrylic	3	0.5 mm	25 μ s
	4	0.5 mm	50 μ s
	5	0.5 mm	75 μ s
Paper	3	0.1 mm	25 μ s
	4	0.1 mm	50 μ s
	5	0.1 mm	75 μ s

Table 5. The calculated and experimental results.

	Pulse number	Calculated		Experiment	
		hole size	hole depth	hole size	hole depth
Acrylic	3	0.518 mm	0.04 mm	0.519 mm	0.042 mm
	4	0.53 mm	0.11 mm	0.528 mm	0.1 mm
	5	0.537 mm	0.18 mm	0.535 mm	0.16 mm
Paper	3	0.118 mm	0.05 mm	0.115 mm	0.045 mm
	4	0.13 mm	0.13 mm	0.12 mm	0.12 mm
	5	0.137 mm	0.20 mm	0.13 mm	0.13 mm

V. Discussion and Conclusion

Through the study of the thermal analysis of laser vaporization, the explicit mathematical expression of shape-drilled is derived. The Formula-deriv-

ved shows the drilled-shape how to take into account some parameters such as power density, pulse duration, pulse waveform, focused beam size, material thermal parameters initial temperature, etc. Meanwhile, the modified laser system is set up to verify the truth of the Formula. We understand the function between shapedrilled and power density is weak, but the strong relation exists between shape-drilled and pulse duration. Then it is expected that the optimal laser pulse for drilling has two characteristics. Firstly, the pulse power density is just higher than the vaporization threshold pulse power density. Secondly, the longer the pulse duration is, the deeper the material will be penetrated. The laser pulse having these two characteristics would vaporize the material effectively, and the laser energy for the removal of materials would be more effectively used.

References

1. K. C. Huang and K. Y. Hsu "New Double-Pulse Excitation Scheme For the $LE\ CO_2$ Lasers" Presented at the first International Symposium on Electronic Devices, IEEE ROC Section, June 1976. It will also be published in the Symposium Proceedings.
2. F. W. Dabby and U. C. Paek, "High-Intensity Laser-Induced Vaporization and Explosion of Solid Material", IEEE J. Quantum Electronics, QE-8, No. 2, 106-111 (February 1972).
3. U. C. Paek and F. P. Gagliano, "Thermal Analysis of Laser Drilling Processes", IEEE J. Quantum Electronics, QE-8, 112-119 (1972).
4. J. F. Ready, "Effects Due to Absorption of Laser Radiation", J. Appl. Phys. 36, 462 (1965).
5. M. K. Chun and K. Rose, "Interaction of High Intensity Laser Beams with Metals", J. Appl. Phys. 41, No. 2, 614-620 (February 1970).
6. H. S. Caslaw and J. C. Jaeger, "Conduction of Heat in Solids", New York, Oxford University Press, 1959.
7. Albert K. Laflamme, "Double Discharge Excitation for Atmospheric Pressure CO_2 Lasers", Rev. Sci. Inst., 41, No. 11, 1578-1581 (November 1970).
8. A. F. Gibson, M. F. Kimmitt, and A. C. Walker, "Photon Drag in Germanium", Appl. Phys. Letters, 17, No. 2, 75-77 (July 1970).
9. G. N. Watson, "A. Treatise on The Theory of Bessel Function", 1941.